Available online at www.sciencedirect.com
SCIENCE DIRECT
Catalysis Today 105 (2005) 134–143
CATALYSIS TODAY
www.elsevier.com/locate/cattod

The relationship between adsorption and solid acidity of heteropolyacids

Michael J. Janik, Robert J. Davis, Matthew Neurock *

Department of Chemical Engineering, University of Virginia, Charlottesville, VA 22904-4741, USA

Abstract

The adsorption energy of a base to a solid acid catalyst is often assumed to correlate with the acid strength of the catalyst. In this study, the influences of adsorbate type, binding configuration and solid acid composition on the adsorption energy are explored using quantum chemical methods. In particular, density functional theory is used to calculate the adsorption energies of functionalized hydrocarbons containing O, N, or S heteroatoms or C=C to phosphotungstic ($H_3PW_{12}O_{40}$) and phosphomolybdic ($H_3PMo_{12}O_{40}$) acids. The adsorption energies of the different molecules bound to the same solid acid are not easily predicted by the proton affinity of the adsorbate because the stabilization of the protonated adsorbate also varies with composition. Bond order conservation helps to explain the relatively small variance in adsorption energies among reactants of widely varying base strength. The activation barriers to form carbenium-ion transition states from adsorbed olefins are also calculated over the two heteropolyacids. The stronger adsorption of propylene to phosphotungstic acid compared to phosphomolybdic acid results in a higher activation barrier to form the carbenium-ion transition state. These heteropolyacids are predicted to have higher activation barriers than zeolites for carbenium-ion formation, which is typically thought to be the rate controlling step in many hydrocarbon conversion processes. This contrasts with the ranking of acid strength based solely on the magnitude of the adsorption energy.

Keywords: Heteropolyacid; Polyoxometalate; Acidity; Adsorption; DFT

1. Introduction

There is a considerable demand for heterogeneous acid catalysts to replace the liquid acids currently used industrially for processes requiring strong acids [1]. For example, the replacement of the homogeneous acid catalysts used to catalyze alkylation reactions (HF and H_2SO_4) will alleviate safety and environmental concerns associated with the handling of these corrosive liquids [2–4]. However, differences between the heterogeneous and homogeneous acids often make substitution of one for the other difficult [5,6]. Heteropolyacids (HPAs) have been shown to catalyze reactions requiring strong acids, for example, the alkylation of isobutane and butene [7,8]. An improved understanding of how reactant and product molecules interact with Brönsted acid sites of HPAs is necessary to develop a rational approach to employing these catalysts. In this paper, quantum chemical calculations are used to examine the general features of the interactions between gas phase species and the HPA catalyst. The adsorption energies of various species and the activation barrier for alkene adsorption are determined.

Heteropolyacids are one of a class of materials known as polyoxometalates [9–11]. HPAs of the Keggin structure ($H_nXM_{12}O_{40}$) are most effective due to a unique combination of their stability, acidity and structural accessibility. The molecular Keggin structure is composed of a central tetrahedron (XO_4^{n-}) surrounded by 12 linked octahedra containing the addenda atoms ($M_{12}O_{36}$). There are four types of oxygen atoms in the Keggin unit, the central oxygen atoms (O_a), corner-sharing bridging oxygen atoms (O_b), edge-sharing bridging oxygen atoms (O_c) and terminal oxygen atoms (O_d). The overall charge of the central tetrahedron is delocalized over the entire structure. Protons associate with the exterior oxygen atoms (O_b, O_c and O_d) and form acidic hydroxyl groups.

* Corresponding author. Tel.: +1 434 924 6248; fax: +1 434 982 2658.
E-mail address: mn4n@virginia.edu (M. Neurock).

0920-5861/$ – see front matter © 2005 Elsevier B.V. All rights reserved.
doi:10.1016/j.cattod.2005.04.014

Phosphotungstic acid ($H_3PW_{12}O_{40}$, HPW) has been shown to be the strongest acid of the heteropolyacids [10–12]. Nevertheless, the ranking of the acid strength of HPW in comparison with other acid catalysts is controversial. Results from Hammett indicators [13] and calorimetric titration in acetonitrile [14] indicated that anhydrous HPW is a superacid. However, other studies have suggested that anhydrous HPW is not a superacid, but has acid strength comparable with zeolites [15,16]. The adsorption energy of basic probe molecules to solid acids is often used to rank acidity. For example, microcalorimetric studies of ammonia [12,17–20] and pyridine [20] adsorption have been used to evaluate the acidity of different HPAs. The stronger adsorption energy of ammonia suggests that HPW is a stronger acid than phosphomolybdic acid ($H_3PMo_{12}WO_{40}$, HPMo) [12,17]. However, the accuracy of using adsorption energies to rank acid strength, and the relationship between adsorption energies and catalyst performance are not fully understood [21,22]. Gorte and co-workers have shown that the deconvolution of chemisorption into a thermodynamic Born cycle comprised of specific elementary processes is a useful framework to examine the individual components which affect the overall adsorption energy (Scheme 1) [23].

In this formalism, adsorption is considered be the result of three processes: the deprotonation of the solid acid; the protonation of the adsorbate and the binding of the protonated adsorbate, or zwitterion, to the conjugate base of the acid. The adsorption energy is expressed as the sum of the catalyst proton affinity (a property of the solid acid), the gas phase proton affinity (a property of the adsorbate), and an interaction energy between the separated ions. Quantum chemical methods can be used to determine the energies of each of these steps, thereby, allowing for the assessment of how each property affects the overall adsorption energy.

In this study, we investigate the adsorption of various reactants or probe species to Keggin structures of different composition. Quantum chemical calculations employing density functional theory (DFT) are used herein to systematically explore the relationship between the base strength of an adsorbate and the energy of adsorption to phosphotungstic acid (HPW). The ability to distinguish the acid strength between HPW and HPMo by the adsorption of various probe molecules is also investigated. In addition, activation barriers for the adsorption of alkenes are determined over both HPW and HPMo, and compared to literature values for adsorption to zeolites. The ranking of acidity by adsorption energies is compared to the predicted performance of the solid acid to catalyze hydrocarbon conversion processes.

2. Computational methods

All of the calculations reported here were performed using non-local gradient corrected plane-wave density functional theory within the Vienna Ab Initio Simulation Package (VASP) [24–26]. The Perdew–Wang (PW91) form of the generalized gradient approximation was used to calculate electron exchange and correlation energies [27]. Vanderbilt ultrasoft pseudopotentials were used to describe electron–ion interactions [28]. A $1 \times 1 \times 1$ Monkhorst–Pack mesh was used to sample the first Brillouin zone [29]. A cut-off energy of 396.0 eV was used to truncate the plane-wave basis sets. The molecular system was represented using a 20 Å × 20 Å × 20 Å unit cell, leaving a minimum of 5 Å of vacuum space between molecules in adjacent unit cells. For charged species, the number of valence electrons was specified and a uniform, neutralizing, background-charge, with its first order energy correction term, was added. The dipole moment between supercells, which results from the homogeneous back-ground charge, was calculated and corrections were added to the total energy [30,31]. Full geometry optimization was performed for each structure examined. These methods have previously been shown to calculate an equilibrium geometry of phosphotungstic acid in agreement with experiment [32]. Transition states were located using the nudged elastic band method as implemented within VASP [33]. The transition state was identified as the image with the highest energy and a tangential force less than 0.08 eV $Å^{-1}$.

The adsorption energy, ΔE_{ads}, is defined as:

$$\Delta E_{ads} = E_{adsorbate/HPA} - E_{HPA} - E_{adsorbate} \quad (1)$$

where $E_{adsorbate/HPA}$ represents the calculated total energy of the adsorbate/HPA system and E_{HPA} and $E_{adsorbate}$ represent the total energies of the separated HPA and adsorbate structures, respectively. The three protons of the heteropolyacid were placed in their optimal positions as previously determined for phosphotungstic acid [32]. To provide a consistent comparison, all adsorbates were considered to interact with a proton on an O_c bridging oxygen site. A negative value of ΔE_{ads} indicates an exothermic adsorption process.

The proton affinity is defined as the negative enthalpy of the reaction $A + H^+ \rightarrow AH^+$ [34]. As defined, the proton affinity is positive. The proton affinity of an acid catalyst is defined such that "A" is the negatively charged catalyst with a proton removed and the "AH^+" species is the neutral

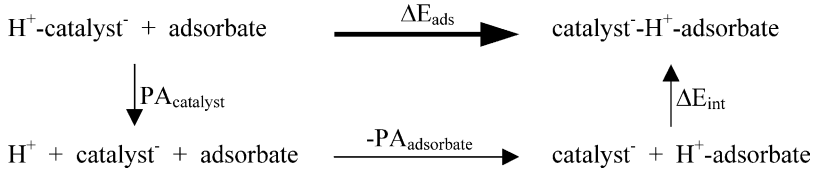

Scheme 1. The thermodynamic cycle for adsorption to a solid acid catalyst [23].

catalyst. The proton affinity of the solid acid catalysts, PA_{HPA}, is defined as:

$$PA_{HPA} = -(E_{HPA} - E_{H^+} - E_{HPA-anion}) \quad (2)$$

The term E_{H^+} represents the calculated energy of an isolated proton and the term $E_{HPA-anion}$ represents the energy of the HPA with one proton removed. For HPW and HPMo, E_{HPA} represents the energy of the neutral structure with three protons bound and $E_{HPA-anion}$ represents the energy of the −1 anion with two protons remaining. In theory, a catalyst with a low proton affinity represents a strong acid, since it refers to a lower energy necessary to remove the proton from the catalyst (less endothermic reaction).

The proton affinity of an adsorbate, PA_{ads}, is defined as:

$$PA_{ads} = -(E_{adsorbate-H^+} - E_{H^+} - E_{adsorbate}) \quad (3)$$

where $E_{adsorbate-H^+}$, represents the energy of the cationic adsorbate structure. An adsorbate which acts as a strong base has a high proton affinity, thus indicating a more exothermic reaction of adding the proton to the base.

The interaction energy, ΔE_{int}, is the energy of adsorbing the protonated adsorbate to the deprotonated HPA, which is defined as:

$$\Delta E_{int} = E_{adsorbate/HPA} - E_{HPA-anion} - E_{adsorbate-H^+} \quad (4)$$

This is also referred to as the zwitterion stabilization energy [35]. In this study, only the interaction of a single adsorbate per Keggin unit is considered. As illustrated in the thermodynamic cycle for adsorption to a solid acid catalyst, the following relationship holds:

$$\Delta E_{ads} = PA_{HPA} - PA_{ads} + \Delta E_{int} \quad (5)$$

Therefore, the adsorption energy of a gaseous species to a solid acid can be examined based on the individual catalyst, adsorbate and their specific interaction characteristics. If the interaction energy were independent of adsorbate, the adsorption energy could be directly predicted as the difference between the catalyst and adsorbate proton affinities.

The energies represented in Eq. (5) were all calculated using gradient corrected density functional theory. Zero-point vibrational energy (ZPVE) corrections were not included in calculating the total energies. While these correction terms predict values that better agree with experiment, they are not necessary to properly evaluate the trends discussed in this study. The calculated values of the PA_{ads} are larger than the experimental values by 20–30 kJ mol^{-1} because they do not consider the change in energy due to the addition of three vibrational modes upon adding a proton to the adsorbate. However, the corrections should not substantially alter the relative proton affinity of the adsorbates considered because C–H, N–H, O–H, or S–H vibrations are of similar energy. As an example, the calculated proton affinity of methanol is 778.6 kJ mol^{-1} before vibrational energy corrections, 738.9 kJ mol^{-1} with ZPVE corrections, and the experimental value is 754.3 kJ mol^{-1} [36]. The inclusion of ZPVE tends to over-correct the energy. The same is true of ammonia, as the calculated proton affinity is 883.5 kJ mol^{-1}, 837.7 kJ mol^{-1} with ZPVE corrections, and the experimental value is 853.6 kJ mol^{-1} [36]. Furthermore, some differences are expected since the experimental proton affinity represents the enthalpy of reaction whereas the calculated values include only the internal energy difference.

3. Results and discussion

3.1. Adsorption to phosphotungstic acid

A common approximation in the literature is to correlate the adsorption energy of a base to a Brönsted acid site directly with the acid site strength. However, as illustrated in Scheme 1, the adsorption energy is a convolution of a distinct acid strength measurement, the acid proton affinity, along with the proton affinity of the base and the zwitterion stabilization energy. In this section, the relationships between the adsorption energy and the last two of these factors are considered by analyzing the adsorption of various bases to a single site of phosphotungstic acid.

The adsorption energies were calculated for various gas phase molecules on phosphotungstic acid (HPW). Adsorbates were chosen that serve as common probes of solid acidity or as reactants in acid-catalyzed reactions. The adsorption energies (ΔE_{ads}), as well as the individual components of the thermodynamic cycle for adsorption on a solid acid ($-PA_{ads}$ and ΔE_{int}), are reported in Table 1. The agreement between the calculated adsorption energies and values measured by microcalorimetry has been previously discussed for the adsorption of ammonia [37] and water [32]. A detailed demonstration of the agreement between computational and experimental adsorption energies of alkenes is published separately [38]. The individual components within the thermodynamic cycle of adsorption on solid acids can be used to better understand the factors which affect the adsorption energy. The calculated proton affinity of HPW is 1080.7 kJ mol^{-1}. Since the solid acid, and therefore, its proton affinity (PA_{HPW}), is constant in Table 1, the adsorption energy differences among the various molecules are due solely to differences between the proton affinity of the adsorbate (PA_{ads}) and the interaction energy of the protonated adsorbate to the anion form of HPW (ΔE_{int}). If ΔE_{int} were constant among the adsorbates, ΔE_{ads} would correlate linearly with PA_{ads}. Fig. 1 compares the adsorption energy to the adsorbate proton affinity. Generally, the adsorption energy becomes more exothermic as the proton affinity, or base strength, of the adsorbate increases. However, there are significant deviations from linearity. Furthermore, though the values of PA_{ads} vary by 270 kJ mol^{-1} among the adsorbates considered, the range of adsorption energies is only 113 kJ mol^{-1}.

The variations from linearity in Fig. 1 are the result of differences in the zwitterion stabilization energies. These

Table 1
Calculated adsorption energies of different molecules to HPW (ΔE_{ads}) and the individual components of the thermodynamic cycle for adsorption[a]

Adsorbate	ΔE_{ads}	$-PA_{ads}$	ΔE_{int}
Ammonia	−129.8	−883.5	−327.0
Methylamine	−156.3	−928.1	−308.9
Dimethylamine	−172.9	−955.8	−297.9
Trimethylamine	−174.4	−972.2	−282.9
Pyridine	−165.4	−962.5	−283.6
2-Fluoropyridine	−104.9	−914.5	−271.2
3-Fluoropyridine	−140.1	−935.6	−285.2
2-Chloropyridine	−125.7	−935.2	−271.2
3-Chloropyridine	−146.9	−940.9	−286.7
2-Methylpyridine	−167.0	−982.2	−265.5
3-Methylpyridine	−173.3	−977.8	−276.2
4-Methylpyridine	−178.0	−982.5	−276.3
Acetonitrile	−83.1	−818.3	−345.6
Methanol	−73.4	−778.6	−375.6
1-Propanol	−74.1	−814.4	−340.5
2-Propanol	−75.9	−826.1	−330.5
Acetone	−85.4	−850.1	−316.0
Water	−67.5	−713.2	−435.0
Methanethiol	−64.7	−801.2	−344.3
Ethane	−86.8	−702.3	−465.2
Propene primary	−76.6	−746.1	−411.2
Propene secondary[b]	−90.3	−783.7	−387.3
1-Butene primary[b]	−88.1	−771.6	−397.3
1-Butene secondary[b]	−102.5	−808.9	−374.4
Trans-2-butene	−79.6	−786.0	−374.4
Isobutene tertiary	−91.4	−844.5	−327.6

All energies in kJ mol^{-1}.
[a] The proton affinity of HPW is 1080.7 kJ mol^{-1}.
[b] Multiple bonding modes of alkene adsorbates were considered to expand the data set. Primary, secondary and tertiary refer to the degree of substitution at the adsorbed carbon.

changes also account for the limited range in the adsorption energies as compared to the much wider range of adsorbate proton affinities. Even without these deviations from linearity, the slope of ΔE_{ads} versus PA_{ads} is still not unity. For example,

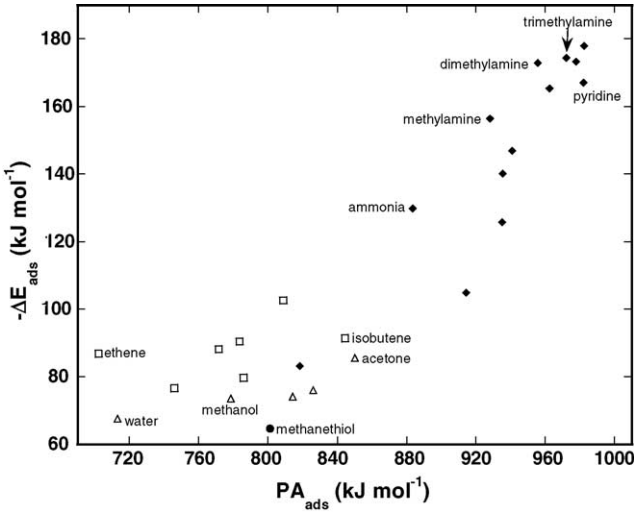

Fig. 1. A comparison of adsorption energy (ΔE_{ads}) vs. adsorbate proton affinity (PA_{ads}) for the adsorption of various species to HPW. (□) Alkenes; compounds which bind through an: (△) oxygen atom, (◆) nitrogen atom, (●) sulfur atom.

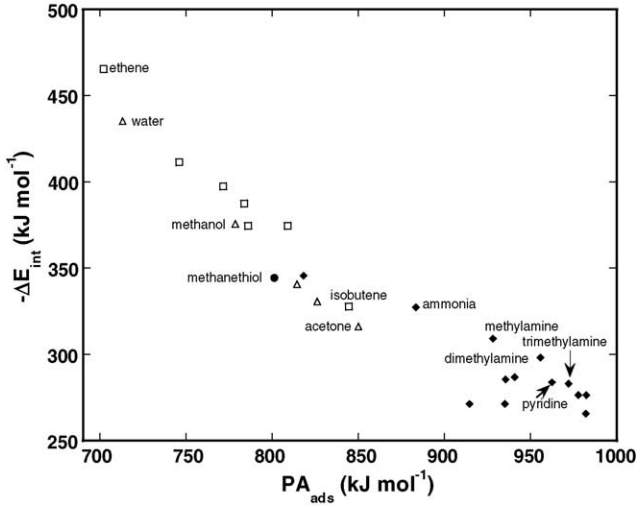

Fig. 2. A comparison of zwitterion stabilization energy (ΔE_{int}) vs. adsorbate proton affinity (PA_{ads}) for the adsorption of various species to HPW. (□) Alkenes; compounds which bind through an: (△) oxygen atom, (◆) nitrogen atom, (●) sulfur atom.

ammonia, methylamine and dimethyl amine show a linear relationship, but with a slope of −0.6 rather than −1. The lower slope is due to the fact that ΔE_{int} changes together with PA_{ads}. Fig. 2 indicates that the interaction energy is linearly correlated with the adsorbate proton affinity, PA_{ads}. The correlation between these two terms can be understood in terms of bond order conservation. The majority of the adsorbates considered herein interact with the acid site by forming a hydrogen bond between the proton of the acid site on the HPW and the heteroatom of the adsorbate (nitrogen, oxygen or sulfur). The proton is then shared between the heteroatom on the adsorbate and the oxygen of HPW as shown in Scheme 2.

Bond order conservation would suggest that the degree of bonding to the proton should be nearly constant. This would imply that as the bond between the proton and the adsorbate (Bond 1 in Scheme 2) weakens, the bond between the zwitterion and the negatively charged HPW structure (Bond 2 in Scheme 2) would strengthen. For a constant catalyst, the strength of Bond 2 is a measurement of the interaction between the proton and the adsorbate and scales with the adsorbate proton affinity. The strength of Bond 1 is the primary component of the zwitterion stabilization energy. Bond order conservation would, therefore, suggest a direct correlation between the adsorbate proton affinity and the zwitterion stabilization energy. As PA_{ads} decreases, ΔE_{int}

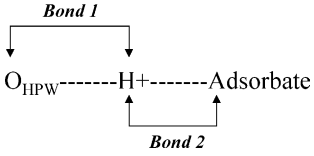

Scheme 2.

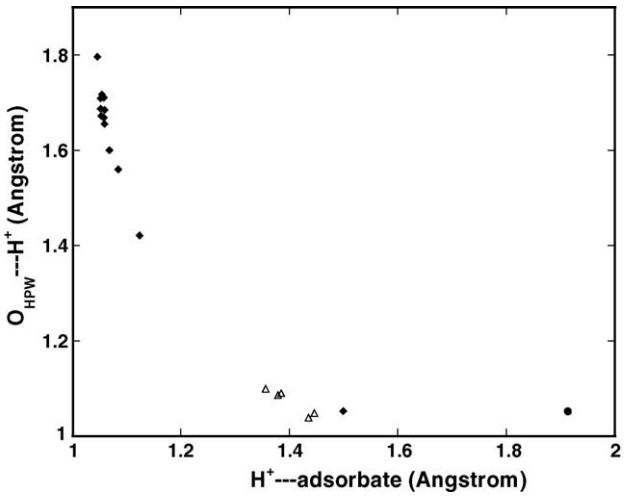

Fig. 3. The bond length between the oxygen atom of phosphotungstic acid and the proton plotted against the bond length between the adsorbate and the proton. The binding geometry is given in Scheme 2. Compounds which bind through an: (△) oxygen atom, (◆) nitrogen atom, (●) sulfur atom.

should increase (become more exothermic). The values of E_{int} vary from −463 to −266 kJ mol^{-1}. The linear relationship between the proton affinity of the adsorbate and the zwitterion stabilization energy would then lead to a systematic decrease in the adsorption energy over the range of proton affinities. Since hydrogen bonding is predominantly comprised of electrostatic interactions, the bond energies should also track with changes in the bond length. Therefore, one might also expect a direct correlation between the $O_{HPW}\cdots H^+$ bond length (Bond 1) and the $H^+\cdots$adsorbate (Bond 2) in Scheme 2. Fig. 3 indeed illustrates the correlation between the $O_{HPW}\cdots H^+$ and the $H^+\cdots$adsorbate bond lengths.

The structure of the adsorbate can also affect the zwitterion stabilization energy with the catalyst surface. Though the primary interaction between most of the adsorbates considered and the catalyst is through the single hydrogen bond of Scheme 2, secondary interactions may contribute to the total interaction energy. Fig. 4 illustrates the optimal adsorption geometry of pyridine to HPW. A single hydrogen bond is formed between the nitrogen atom of pyridine and a proton atom at an O_c site on HPW. The hydrogen atoms at the carbon positions ortho to the nitrogen atom are ∼2.27 Å away from the terminal oxygen atoms of the Keggin unit, which may result in weak attractive interactions. Rotating the adsorbed pyridine 90° about the N–H bond leads to a structure which is 11.1 kJ mol^{-1} less favorable, indicating that rotation indeed removes these weak attractive interactions. Similarly, adsorbates that contain an electron deficient hydrogen atom may bond in a bidentate mode, in which two hydrogen bonds are formed. For example, the bidentate mode of adsorption is preferred for ammonia (Fig. 5). The first hydrogen bond is between a hydroxyl group on the Keggin structure and the nitrogen atom of the adsorbate. The second is between a hydrogen atom bound to the adsorbate and a second oxygen atom (O_d)

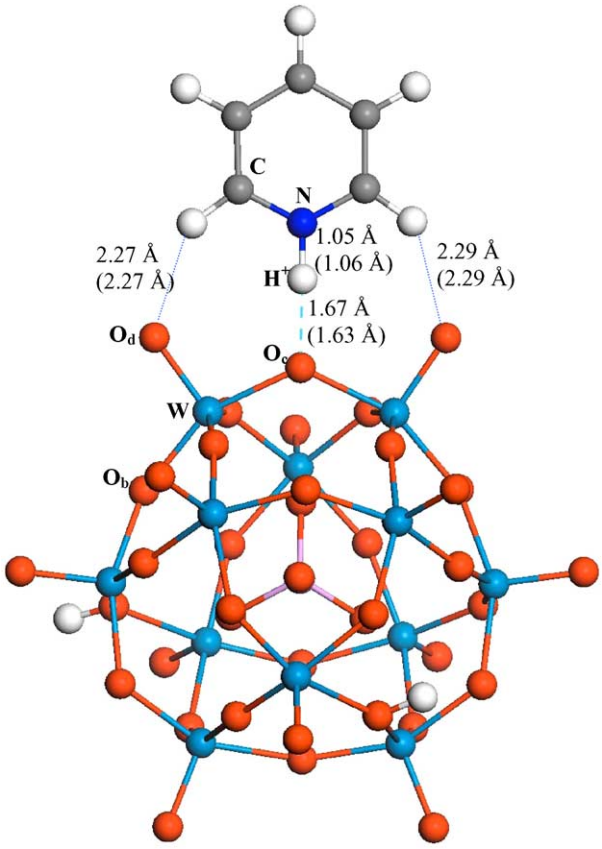

Fig. 4. Pyridine adsorbed to a proton on an O_c site of HPW. A hydrogen bond is formed between the nitrogen of pyridine and the O_c atom. The adsorption energy is −165.4 kJ mol^{-1}. Distances shown in parentheses are for adsorption to HPMo.

at the Keggin surface. Bidentate adsorption is also preferred for other protic type adsorbates including water, methanol, methanethiol, methylamine and dimethylamine.

Deviations from linearity are also observed in Fig. 2 within groups of species that have a common primary interaction with HPW. For example, the interaction energy does not correlate linearly with adsorbate proton affinity within the group of species that adsorb primarily through a proton–nitrogen hydrogen bond. The interaction energies of ammonia, methylamine and dimethylamine are larger than those of substituted pyridines of similar PA_{ads}. This is likely due to differences in secondary interactions, as methylamine and dimethylamine bond in a bidentate mode, thus forming an additional hydrogen bond. The interaction energy of trimethylamine indicates the inability to form a second hydrogen bond. Within the pyridine series, those species substituted at the two position show a relatively weaker (less exothermic) interaction energy due to the repulsion between the chlorine, fluorine, or methyl group and the oxygen atoms of HPW. In fact, the optimal adsorbed state of these species requires rotation of the adsorbate 90° about the N–H bond, or out of the plane of Fig. 4. The substitution and rotation removes the favorable interaction of the pyridine H atoms and the O_d atoms of HPW.

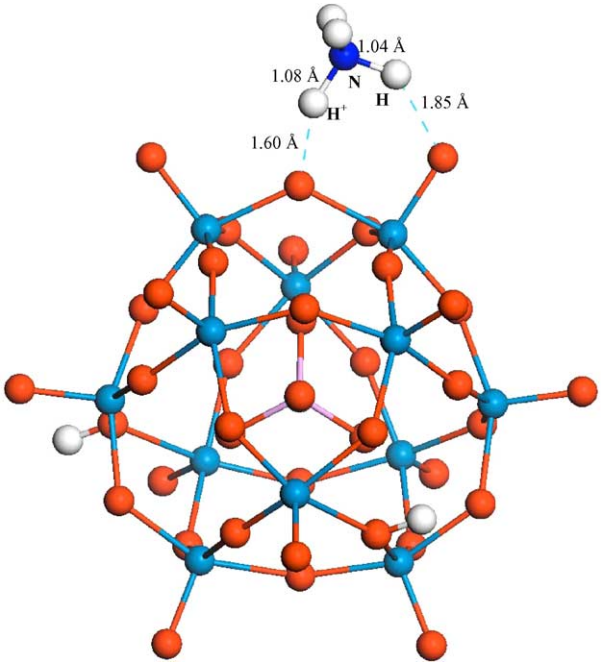

Fig. 5. Ammonia adsorbed bidentate to O_c and O_d atoms of HPW. Hydrogen bonds are formed between the nitrogen of ammonia and a proton on an O_c atom and between a hydrogen atom from ammonia and an O_d atom of HPW. The adsorption energy is -129.8 kJ mol^{-1}.

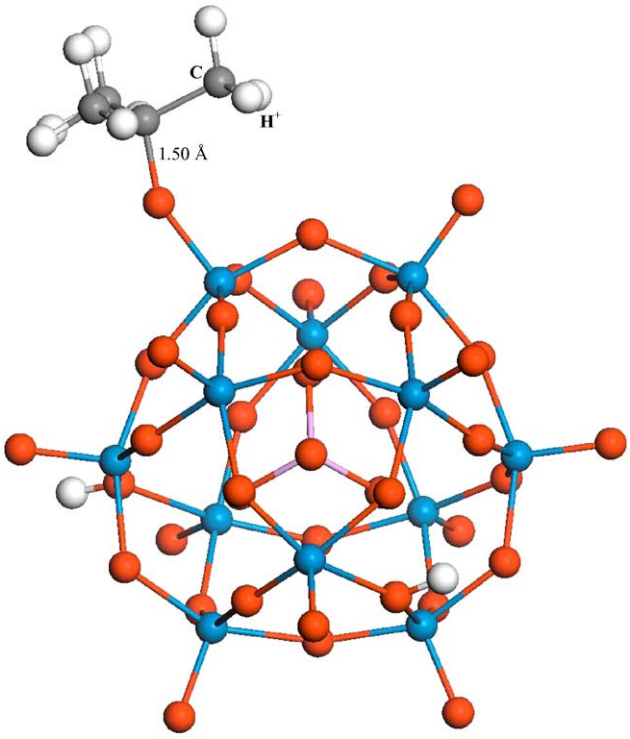

Fig. 6. Isobutene adsorbed to form an alkoxy species bound to an O_d atom of HPW. The acidic proton (originally bound to an adjacent O_c atom of HPW) is added to the primary carbon of the isobutylene double bond, and the tertiary carbon forms a covalent bond with the O_d atom of HPW. The adsorption energy is -91.4 kJ mol^{-1}.

Despite the deviations mentioned, there are homologous series which show a linear correlation between the adsorption energy and the adsorbate proton affinity. These series of molecules have common primary and secondary interactions with HPW. For example, ammonia, methylamine and dimethylamine represent such a homologous series. The pyridine species that are not substituted at the two-position represent a second homologous series. However, as illustrated above, the slope of ΔE_{ads} versus PA_{ads} for a homologous series is not unity due to the correlation of ΔE_{int} with PA_{ads}.

The chemisorption of alkenes does not occur through hydrogen bonding, and therefore, the analysis above does not apply directly. A detailed discussion of the factors, which influence the adsorption energies of alkenes to phosphotungstic acid is published elsewhere [38]. The adsorption of alkenes occurs by donation of the proton to one carbon atom of the double bond with the other carbon atom forming a covalent bond with an O_d atom of HPW. The adsorbed state of isobutene is illustrated in Fig. 6. For the adsorption of alkenes, there is no discernable trend for the adsorption energy with respect to the adsorbate proton affinity. The ΔE_{int} values are somewhat linear with PA_{ads} (Fig. 2), indicating that the interaction energy is directly related to the adsorbate proton affinity though the adsorption energy is not.

In summary, the adsorption energies for different reactants to a solid acid do not directly correlate with their proton affinities. The zwitterion stabilization energy becomes more exothermic as the adsorbate proton affinity increases, thereby decreasing the adsorption energy variation between adsorbates. This is the direct result of bond order conservation: the total bond energy between the proton and the adsorbate and the proton and the anionic substrate remains relatively constant despite deviations in the adsorbate proton affinity. This trend reduces the deviation of the adsorption energies of different species due to the primary binding interaction. Coupled with differences in the secondary interactions between adsorbates and the catalyst surface, gas phase species of different base strength may show remarkably similar adsorption energies.

3.2. Adsorption to phosphomolybdic acid

The thermodynamic cycle of adsorption to a solid acid also provides a useful framework in which to consider the ability of adsorption to differentiate the acid strength between catalysts. For this purpose, the adsorption energies of various probe or reactant molecules to phosphomolybdic acid (HPMo) were calculated. Previous results indicated that changing the addenda atoms from tungsten to molybdenum decreases the acid strength of the heteropolyacid [12]. The calculated proton affinity of HPMo was found to be 1103.4 or 22.7 kJ mol^{-1} greater than that of HPW. The change of addenda atoms does not change the number of protons per Keggin unit. The positions of the protons and the binding site for the adsorbates are chosen to be the same as for HPW.

Table 2
Calculated adsorption energies of different molecules to HPMo (ΔE_{ads})

Adsorbate	PA_{ads}	ΔE_{ads}	$\Delta(\Delta E_{ads})$	$\Delta(\Delta E_{int})$
Pyridine	−962.5	−143.7	21.7	−1.0
Ammonia	−883.5	−116.5	13.3	−9.4
Acetone	−850.1	−74.8	10.6	−12.1
2-Propanol	−826.1	−65.4	10.5	−12.1
1-Propanol	−814.4	−64.6	9.5	−13.2
Methanethiol	−801.2	−54.0	10.6	−12.0
Trans-2-butene	−786.0	−64.4	15.3	−7.4
Propene secondary	−783.7	−70.4	19.9	−2.7
Methanol	−778.6	−69.1	4.4	−18.3
Water	−713.2	−59.4	8.1	−14.6

The differences in the adsorption energies, $\Delta(\Delta E_{ads})$, and interaction energies, $\Delta(\Delta E_{int})$, between HPW and HPMo are given. All values are in kJ mol^{-1}.

The adsorption energies of various species to HPMo are given in Table 2, along with the changes in adsorption energies, $\Delta(\Delta E_{ads})$, and interaction energies, $\Delta(\Delta E_{int})$, between HPMo and HPW. If the zwitterion stabilization energies did not differ between catalysts, the adsorption to HPMo would be 22.7 kJ mol^{-1} less exothermic. However, as HPMo is a weaker acid than HPW, the conjugate base of HPMo is stronger than that of HPW. Therefore, the interaction of the deprotonated HPMo with the protonated adsorbate is more exothermic. This leads to an overall adsorption energy on HPMo which is more exothermic than would be predicted based on the proton affinity difference between HPMo and HPW. The stronger interaction of the protonated adsorbate with HPMo is evident from the adsorption geometries. For example, the $N–H^+–O^{\delta-}$ distance for pyridine adsorption to HPMo (Fig. 4) and the $C–O_d$ bond of secondary butene adsorption to HPMo are slightly shorter than the same configuration involving HPW.

Depending on the acid-catalyzed process being considered, a stronger zwitterion stabilization energy may not be beneficial to the performance of the catalyst. For example, the strongly bound alkoxy intermediate that forms as a result of hydrocarbon adsorption may make the subsequent transformation processes of alkylation or isomerization more difficult, as they require breaking the C–O bond. However, this stronger interaction energy serves to increase the adsorption energy, thereby blurring the differences between solid acids. As the proton affinity difference between HPW and HPMo is small, this effect appears to be minor. In zeolites, however, the proton affinity is typically on the order of 1250 kJ mol^{-1} [39], and the butene adsorption energy is approximately 60 kJ mol^{-1} [40]. This results in a zwitterion stabilization energy of −524 kJ mol^{-1}, which is 150 kJ mol^{-1} stronger than that of HPW. The 170 and 150 kJ mol^{-1} differences in the catalyst proton affinities and zwitterion stabilization energies, respectively, between zeolites and heteropolyacids are not apparent in the overall adsorption energy difference of 20 kJ mol^{-1}. The implications of differences in the adsorption energy and interaction energy on catalyst performance can not be determined without the consideration of the transition state for the conversion process and its interaction with the catalyst.

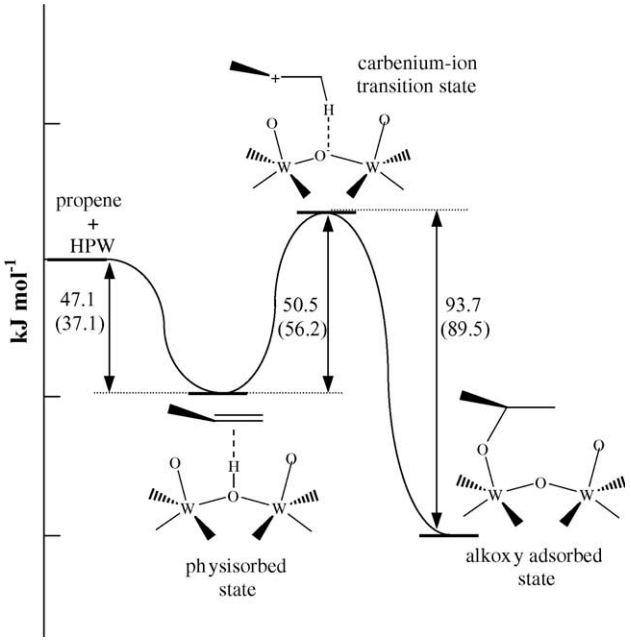

Fig. 7. Plot of the reaction profile for propene adsorption to an HPA. The energies given for adsorption to HPW, whereas the values in parentheses refer to adsorption onto HPMo.

3.3. Activation barriers for adsorption of propene

The reaction profile for the adsorption of propene on both HPW and HPMo is illustrated in Fig. 7. The alkene initially adsorbs as a physisorbed π-complex in which electron density from the carbon–carbon double bond interacts in a manner similar to formation of an adsorbate–proton hydrogen bond. Conversion to the chemisorbed alkoxy state occurs by the donation of the proton to one end of the double bond of the alkene and the formation of a C–O bond between the other carbon of the double bond and an oxygen atom of the HPA. The energetics of alkene adsorption have been studied computationally over Brönsted acid sites of zeolites [41,42]. The transition state for chemisorption resembles a carbenium-ion, with the new C–H bond almost completely formed at the transition state while the alkoxy bond has not yet formed. The transition state for propene adsorption to HPW for a secondary alkoxy bond is illustrated in Fig. 8.

The activation barrier for adsorption of propene to HPW (Fig. 7) is 50.5 kJ mol^{-1} and the barrier for adsorption to HPMo is 56.2 kJ mol^{-1}. The activation barrier is given as the difference in energy between the physisorbed π-complex and the transition state. The activation barrier is similar to that calculated using similar methods for the adsorption of propene over chabazite (Si:Al, 11:1), 56 kJ mol^{-1} [42]. The

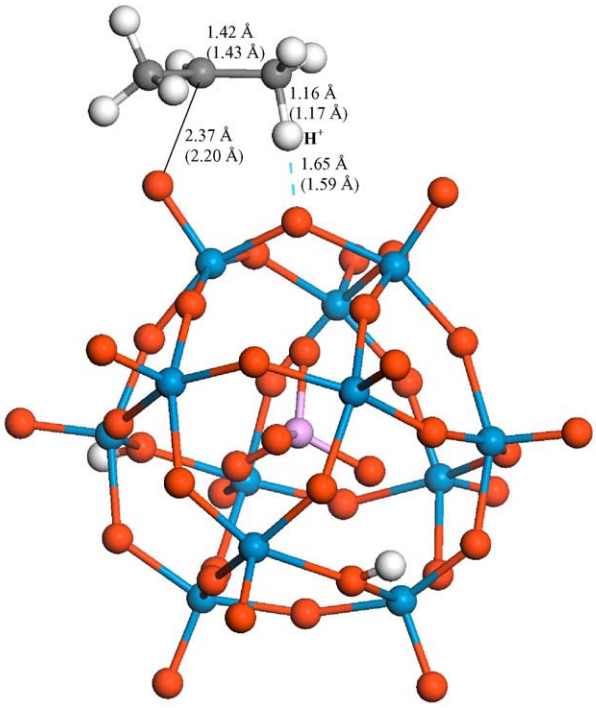

Fig. 8. The transition state for the secondary adsorption of propene to HPW. Distances in parentheses are for the same state over HPMo. The activation barrier to adsorption is 50.5 kJ mol^{-1} on HPW and 56.2 kJ mol^{-1} on HPMo.

activation barrier may be viewed as the difference in interaction energy of the physisorbed state and the transition state with the catalyst (Scheme 3).

In this formalism, the transition state can be viewed as an adsorbed state with an interaction defined as in Eq. (4). Rozanska et al. report an adsorption energy of −21 kJ mol^{-1} for the physisorbed state on chabazite [42]. Though the physisorption energy indicates a larger difference between the HPAs and chabazite, the activation barriers are quite similar as they involve two ''adsorbed'' states of the same species, the π-complex and the transition state. The relative energy of the transition state compared to the separated HPA and gas phase species is substantially lower over the HPAs than over chabazite. However, as the activation energy requires the comparison of two states interacting with the catalyst, this difference would likely not be apparent in the rate of conversion from the physisorbed to chemisorbed states.

The reverse reaction of alkene adsorption, the conversion of an adsorbed alkoxy species to the carbenium-ion transition state, is hypothesized to be the rate limiting step

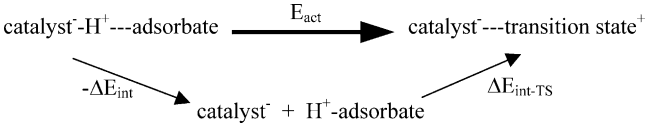

Scheme 3.

in many hydrocarbon conversion processes. For example, the formation of the carbenium-ion transition state complex from the adsorbed alkoxy state is proposed to be the rate controlling step of alkene double bond shift, skeletal isomerization, cracking and oligomerization [43]. The activation barrier for the desorption of the chemisorbed propene is 93.7 kJ mol^{-1} from HPW and 89.5 kJ mol^{-1} from HPMo. The activation barrier to the formation of a carbenium-ion transition state is lower over HPMo than over HPW. It must be noted that the difference between these two catalysts is small, and therefore, should not be taken as conclusive evidence of HPMo's superiority as an acid catalyst. The activation barrier to form the transition state from the alkoxy species for *trans*-2-butene is 84.6 kJ mol^{-1} over HPW and 86.9 kJ mol^{-1} over HPMo, suggesting a similar performance of the two acids. Other factors, such as the relative thermal stability of HPW and HPMo, may also impact their performance as acid catalysts. However, comparing activation barriers and adsorption energies between the two catalysts provides conflicting predictions of acid strength.

Depending on the energy of forming the alkoxy state, a solid acid classified as weaker by a ranking of adsorption energies may show a smaller activation barrier for the desorption of the alkoxy species. The chemisorption energy of propene to chabazite was reported to be −48 kJ mol^{-1} [42]. This is substantially weaker than that of propene on HPW, which is −90.3 kJ mol^{-1}. Therefore, propene desorption will have a substantially higher activation barrier over HPW than over chabazite. For a reaction in which the rate controlling step is the formation of a secondary carbenium-ion transition state, a zeolite may show an intrinsically higher reaction rate than an HPA, despite the HPA being ranked as a stronger acid based on the adsorption energy of a basic probe molecule. This is likely to hold under conditions producing high intermediate coverages in which the overall rate is proportional to the rate constant of the rate-limiting step.

According to Scheme 3, a lower activation barrier for a hydrocarbon conversion process over a solid acid is obtained when the interaction energy of the transition state is closest to the interaction energy of the adsorbed equilibrium state. A

Table 3
Adsorption energies of the physisorbed state, carbenium-ion transition state and chemisorbed state of propene on the zeolite chabazite, HPW and HPMo

State	Chabazite[a] (kJ mol^{-1})		HPW (kJ mol^{-1})		HPMo (kJ mol^{-1})	
	ΔE_{ads}	ΔE_{int}	ΔE_{ads}	ΔE_{int}	ΔE_{ads}	ΔE_{int}
π-Complex	−21	−427	−47	−344	−37	−357
Carbenium TS[b]	+35	−371	+3	−294	+19	−301
Alkoxy	−48	−454	−90	−387	−70	−390

[a] Data from Rozanska et al. [42]. Proton affinity of chabazite taken as 1190 kJ mol^{-1} [43].

[b] Adsorption energy of the carbenium-ion transition state given compared to the separated alkene and catalyst species to allow direct comparison between states.

comparison of our calculations of the alkene adsorption energetics over HPAs and those of Rozanska et al. [42] indicates that the interaction energies of both alkoxy and transition states are higher over chabazite than over HPW. However, the activation barrier for formation of the transition state from the alkoxy species is lower over the zeolite due to the relative interaction energies. To provide a direct comparison, values for the physisorbed, transition and chemisorbed states for the secondary adsorption of propene are compared among HPW, HPMo and chabazite in Table 3. In calculating interaction energies, the proton affinity of chabazite was taken as 1190 kJ mol^{-1} [44]. Though a comparison of proton affinities and adsorption energies would indicate that HPW is a stronger acid, the relative stability of the transition state may lead to chabazite acting as the better acid catalyst for certain hydrocarbon conversion processes.

4. Summary and conclusions

The adsorption energies of various probe and reactant molecules were calculated for adsorption to phosphotungstic acid and phosphomolybdic acid using ab initio quantum chemical methods. The adsorption energy could not be directly predicted by the knowledge of the relative catalyst and adsorbate proton affinities because of variations in the energy of interaction of the adsorbate and the acid. Variations in this zwitterion stabilization energy among adsorbates on a given solid acid result from differences in the binding mode of adsorbates as well as the trend of decreasing interaction energies with increasing adsorbate proton affinities. Changes in the interaction energies between the same adsorbate and different catalysts make differentiation of solid acid strengths between catalysts difficult. Small differences in the adsorption energy of a probe to various catalysts may mask large differences in the acidic properties of the solid. Furthermore, stronger adsorption energies may not be indicative of a better acid catalyst. Since the activation barrier of hydrocarbon conversion processes over solid acids is determined by the relative energy of adsorbed and transition states, a stronger adsorption may lead to a less active catalyst. This was demonstrated here by comparing the energetics of secondary propene adsorption to heteropolyacids and acidic chabazite. The activation barrier for the conversion of the adsorbed alkoxy species to the carbenium-ion transition state over phosphomolybdic acid is slightly lower than that over phosphotungstic acid, despite a prediction from trends in adsorption energies of phosphomolybdic acid being a weaker acid. Comparison with values from the literature for chabazite suggests that the activation barrier over zeolites is substantially lower than that over phosphotungstic acid because of a stronger adsorption of the alkoxy species on the heteropolyacids.

Acknowledgements

We are grateful for the support of the National Science Foundation (CTS-0124333) for funding this research. We also thank the Environmental Molecular Science Laboratory at Pacific Northwest Laboratories (Project 3568) for computational support.

References

[1] J. Weitkamp, Y. Traa, Catal. Today 49 (1999) 193.
[2] K. Tanabe, W.F. Holderich, Appl. Catal. A 181 (1999) 399.
[3] S.I. Hommeltoft, Appl. Catal. A 221 (2001) 421.
[4] R.A. Sheldon, R.S. Downing, Appl. Catal. A 189 (1999) 163.
[5] D.J. Parillo, R.J. Gorte, W.E. Farneth, J. Am. Chem. Soc. 115 (1993) 12441.
[6] W.E. Farneth, R.J. Gorte, Chem. Rev. 95 (1995) 615.
[7] P.Y. Gayraud, I.H. Stewart, S.B. Derouane-Abd Hamid, N. Essayem, E.G. Derouane, J.C. Vedrine, Catal. Today 63 (2000) 223.
[8] T. Blasco, A. Corma, A. Martinez, P. Martinez-Escolano, J. Catal. 177 (1998) 306.
[9] M.T. Pope, Heteropoly and Isopoly Oxometalates, Springer-Verlag, New York, 1983.
[10] T. Okuhara, N. Mizuno, M. Misono, Adv. Catal. 41 (1996) 113.
[11] I.V. Kozhevnikov, Russ. Chem. Rev. 56 (1987) 811.
[12] B.B. Bardin, S.V. Bordawekar, M. Neurock, R.J. Davis, J. Phys. Chem. B 102 (1998) 10817.
[13] T. Okuhara, T. Nishimura, H. Watanabe, M. Misono, J. Mol. Catal. 74 (1992) 247.
[14] R.S. Drago, J.A. Dias, T.O. Maier, J. Am. Chem. Soc. 119 (1997) 7702.
[15] C. Paze, S. Bordiga, A. Zecchina, Langmuir 16 (2000) 8139.
[16] N. Essayem, G. Coudurier, J.C. Vedrine, D. Habermacher, J. Sommer, J. Catal. 183 (1999) 292.
[17] L.C. Jozefowicz, H.G. Karge, E. Vasilyeva, J.B. Moffat, Microporous Mater. 1 (1993) 313.
[18] F.X. Liu-Cai, B. Sahut, E. Faydi, A. Auroux, G. Hervé, App. Catal. A: Gen. 185 (1999) 75.
[19] F. Lefebvre, F.X. Liu-Cai, A. Auroux, J. Mater. Chem. 4 (1994) 125.
[20] E.F. Kozhevnikova, I.V. Kozhevnikov, J. Catal. 224 (2004) 164.
[21] C. Lee, D.J. Parrillo, R.J. Gorte, W.E. Farneth, J. Am. Chem. Soc. 118 (1996) 3262.
[22] R.J. Gorte, D. White, Top. Catal. 4 (1997) 57.
[23] M.T. Aronson, R.J. Gorte, W.E. Farneth, J. Catal. 98 (1986) 434.
[24] G. Kresse, J. Hafner, Phys. Rev. B 47 (1993) 558.
[25] G. Kresse, J. Furthmuller, Comput. Mater. Sci. 6 (1996) 15.
[26] G. Kresse, J. Furthmuller, Phys. Rev. B 54 (1996) 11169.
[27] J.P. Perdew, J.A. Chevary, S.H. Vosko, K.A. Jackson, M.R. Pederson, D.J. Singh, C. Fiolhais, Phys. Rev. B 46 (1992) 6671.
[28] D. Vanderbilt, Phys. Rev. B 41 (1990) 7892.
[29] H.J. Monkhorst, J.D. Pack, Phys. Rev. B 13 (1976) 5188.
[30] G. Makov, M.C. Payne, Phys. Rev. B 51 (1995) 4014.
[31] J. Neugebauer, M. Scheffler, Phys. Rev. B 46 (1992) 16067.
[32] M.J. Janik, K.A. Campbell, B.B. Bardin, R.J. Davis, M. Neurock, Appl. Catal. A 256 (2003) 51.
[33] G. Mills, H. Jonsson, G.K. Schenter, Surf. Sci. 324 (1995) 305.
[34] J.W. Keister, J.S. Riley, T. Baer, J. Am. Chem. Soc. 115 (1993) 12613.
[35] R.A. van Santen, G.J. Kramer, Chem. Rev. 95 (1995) 637.
[36] E.P. Hunter, S.G. Lias, in: P.J. Linstrom, W.G. Mallard (Eds.), NIST Standard Reference Database Number, vol. 69, National Institute of Standards and Technology, Gaithersburg, MD, 2003.
[37] B.B. Bardin, R.J. Davis, M. Neurock, J. Phys. Chem. B 104 (2000) 3556.

[38] K.A. Campbell, M.J. Janik, R.J. Davis, M. Neurock, Langmuir 21 (2005) 4738.
[39] G.J. Kramer, R.A. van Santen, J. Am. Chem. Soc. 115 (1993) 2887.
[40] L. Benco, J. Hafner, F. Hutschka, H. Toulhoat, J. Phys. Chem. B 107 (2003) 9756.
[41] A. Bhan, Y.V. Joshi, W.N. Delgass, K.T. Thomson, J. Phys. Chem. B 107 (2003) 10476.
[42] X. Rozanska, T. Demuth, F. Hutschka, J. Hafner, R.A. van Santen, J. Phys. Chem. B 106 (2002) 3248.
[43] V.B. Kazansky, Catal. Today 51 (1999) 419.
[44] M. Brandle, J. Sauer, J. Am. Chem. Soc. 120 (1998) 1556.